Determination of Bond Distances and Bond Angles by Solid-State Nuclear Magnetic Resonance. ^{13}C and ^{14}N NMR Study of Glycine

R. A. Haberkorn, R. E. Stark, H. van Willigen, and R. G. Griffin*

Contribution from the Francis Bitter National Magnet Laboratory, Massachusetts Institute of Technology, Cambridge, Massachusetts 02139. *Received September 15, 1980*

Abstract: C-C and C-N bond distances and the C-C-N angle in glycine were determined from ^{13}C-^{13}C and ^{13}C-^{14}N dipolar splittings in single-crystal ^{13}C NMR spectra. The measured values (r_{CC} = 1.543 ± 0.008 Å, r_{CN} = 1.509 ± 0.009 Å, and ∠CCN = 111.1 ± 1.0°) are in excellent agreement with neutron diffraction results. ^{13}C shift tensors for $-CH_2-$ and $-CO_2^-$ and their molecular orientations are also reported. ^{14}N NMR spectra are presented which illustrate the increased resolution available from studies of $I > 1/2$ nuclei, and they also allow the determination of the ^{14}N quadrupole coupling constant and its asymmetry. We find e^2qQ/h = 1.18 ± 0.01 MHz and η = 0.54 ± 0.01 with V_{ZZ} approximately along the C-N bond and V_{XX} almost perpendicular to the CCN plane.

Introduction

The past few years have witnessed the development of several methods for performing high-resolution nuclear magnetic resonance experiments in solids. These include multiple-pulse techniques,[1,2] which are applicable to homonuclear dipolar broadened spin systems, as well as double resonance techniques[2,3] for the direct and indirect detection of dilute spin resonances. The main thrust of these techniques is the elimination of hetero- and homonuclear dipolar couplings which are the main source of line broadening in solids. For this purpose the double resonance technique of Pines, Gibby, and Waugh[3] has proven to be particularly useful as it is easy to implement experimentally, has relatively high sensitivity, and is applicable to a wide variety of interesting chemical, physical, and biological problems.

The underlying strategy of this experiment is to remove heteronuclear interactions, from protons in the lattice, by strong decoupling fields and to attenuate homonuclear dipolar couplings via the r^{-3} dependence of this interaction. Originally, isotopic dilution was utilized to accomplish this, but magnetic dilution is, in fact, a much more generally occurring phenomenon. In particular, many isotopes which are ~100% abundant, such as ^{31}P and ^{14}N, usually satisfy criteria for being magnetically dilute since they occur in a lattice rich in nonmagnetic nuclei, e.g., ^{16}O and/or ^{12}C. In addition, since homonuclear broadening is proportional to γ^2 of these nuclei, the size of the homonuclear dipolar term is attenuated further. Therefore, for many compounds of interest the criteria for magnetic dilution are satisfied without any special precautions. For the same reason, enriched compounds exhibit solid-state NMR spectra which are essentially free from severe broadening effects.

Even though the elimination of dipolar couplings is responsible for the improved resolution observed in NMR spectra of solids, the early work of Pake[4] established that structural information could be obtained by observing dipolar splittings. In particular, the form of the dipolar Hamiltonian[4,5] is well defined and contains explicitly the length and orientation of the vector joining the two interacting nuclei. Therefore, determination of dipolar couplings provides directly structural information such as bond lengths and angles. Moreover, because of the simplicity of the NMR experiment, one is tempted to try to recover these couplings in order to extract such information. Fortunately, certain spin pairs such as ^{13}C-^{14}N, ^{14}N-^{1}H, and ^{13}C-^{1}H are ubiquitous in nature and for reasons discussed above are magnetically dilute; thus, the corresponding dipolar couplings have been observed in a number of cases.[6-11] Use of dipolar couplings, therefore, shows promise as a precise and simple method for determining bond distances and angles and, when sufficient information is available, the overall molecular structure. We demonstrate this method with single-crystal studies of the simple amino acid, glycine, in which we have determined the C-C and C-N bond distances as well as the C-C-N angle from C-C and C-N dipolar spectra. In addition, we also report data for the ^{13}C shift tensors in this molecule.

As the molecules we wish to study become more complex, so do the corresponding NMR spectra and the consideration of resolution quickly becomes an important issue. Therefore any improvement in the attainable resolution is accompanied by a similar increase in the ability to study systems of higher complexity. At present, line widths for solid-state ^{13}C spectra are typically of the order of ~100 Hz, and for carboxyl or aromatic carbons the chemical shift anisotropy can be as high as 150 ppm[12] or ~11 kHz on our 6.8 T spectrometer. This situation results in resolution of $\Delta/\Delta\nu \approx 100$, where Δ is the total spectral breadth and $\Delta\nu$ is the line width. However, if we turn our attention to measuring ^{14}N resonances, we note that the ^{14}N quadrupole couplings can be as large as 1-3 MHz,[10,13] thus spreading the spectrum over a range of as much as 4.5 MHz. Although the line widths in ^{14}N spectra are typically an order of magnitude greater than for ^{13}C, the resolution is almost two orders of magnitude greater, $\Delta/\Delta\nu \approx 5 \times 10^3$, which is comparable with the resolution attainable with ^{13}C solution NMR spectra. In addition, we should also point out that ^{14}N is 99.4% abundant, permitting spectra to be obtained in relatively short periods of time. Again using glycine as an example, we demonstrate these two points with a determination of the ^{14}N quadrupole coupling constant for the $-NH_3^+$ group in this simple molecule.

(1) U. Haeberlaen, "High Resolution NMR in Solids, Selective Averaging", Academic Press, New York, 1976.
(2) M. Mehring, "High Resolution NMR Spectroscopy in Solids", Vol. 11, P. Diehl, E. Fluck, and R. Kosfeld, Eds., Springer-Verlag, New York, 1976.
(3) A. Pines, M.G. Gibby, and J.S. Waugh, *J. Chem. Phys.*, **59**, 569 (1973).
(4) G. E. Pake, *J. Chem. Phys.*, **16**, 327, (1948).
(5) A. Abragam, "The Principles of Nuclear Magnetism", Oxford University Press, Oxford, 1961, pp 103-4.
(6) R. G. Griffin, A. Pines, and J. S. Waugh, *J. Chem. Phys.*, **63**, 3676 (1975).
(7) M. E. Stoll, R. W. Vaughan, R. B Saillant, and T. Cole, *J. Chem. Phys.*, **61**, 2896 (1974).
(8) R. K. Hester, J. L. Ackerman, B. L. Neff, and J. S. Waugh, *Phys. Rev. Lett.*, **36**, 1081 (1976).
(9) M. E. Stoll, A. J. Vega, and R. W. Vaughan, *J. Chem. Phys.*, **65**, 4093 (1976).
(10) R. E. Stark, R. A. Haberkorn, and R. G. Griffin, *J. Chem. Phys.*, **68**, 1996 (1978).
(11) H. van Willigen, R. G. Griffin, and R. A. Haberkorn, *J. Chem. Phys.*, **67**, 5855 (1977).
(12) See, for instance, ref 2, Chapter 5.
(13) E.A.C. Lucken, "Nuclear Quadrupole Coupling Constants", Academic Press, New York, 1969, Chapter 11.

0002-7863/81/1503-2534$01.25/0

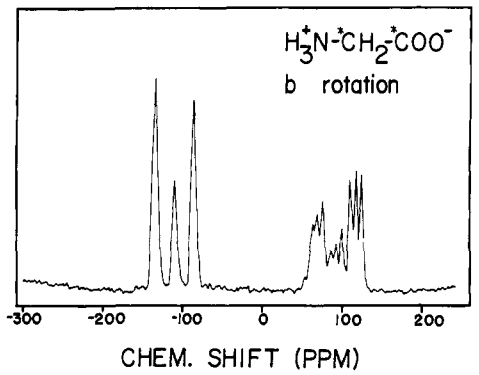

Figure 1. ^{13}C NMR spectrum of a single crystal of glycine with 9% [1,2-$^{13}C_2$]glycine. The *b* crystallographic axis is perpendicular to the magnetic field, B_0. The *a* axis was approximately parallel with B_0.

Experimental Section

Single crystals of glycine and 9% [1,2-$^{13}C_2$]glycine (Koch Isotope) were grown by slow evaporation from aqueous solution. Crystal morphology was used to optically orient the samples on the goniometer in the NMR probe. Orthogonality of the rotation planes was verified by examining their angles of interception. All spectra were recorded in the presence of a 12-G proton decoupling field on a home-built spectrometer operating at 6.8 T (ν_{1H} = 294 MHz). Standard cross polarization[3] and Fourier transform techniques were used to improve the signal-to-noise ratio. The B_1 rf fields used for the cross polarization were 40 G for ^{13}C (ν_0 = 73.96 MHz), and 140 G for ^{14}N (ν_0 = 21.25 MHz) with a 10-G proton field in each case. Spectra with excellent signal to noise were obtained after averaging 100–200 transients (~1–3 min).

Results

The conditions used for the crystal growth favored the formation of the α modification of glycine which crystallizes in the monoclinic space group $P2_1/n$ with four molecules in the unit cell and two molecules in the asymmetric unit.[14] Therefore, in a general orientation there are two magnetically inequivalent molecules per unit cell, and two different sets of NMR signals will be observed. However, the molecules are also related by a mirror plane[15] containing the *a* and *c* crystal axes, and when the static magnetic field, B_0, is parallel to the *ac* plane, all molecules in the unit cell are magnetically equivalent and only one set of resonances will be observed. The magnitude of each principal component of any tensor, e.g., chemical shift, dipolar, or quadrupolar coupling, will be equal for all four molecules, but the direction of each of these components will be related by the symmetry operations of the unit cell. That is, the direction cosines in the crystal frame for one component of a tensor for one molecule will be related to the similar components for the other three molecules by the relations XYZ, $X\bar{Y}Z$, $\bar{X}\bar{Y}\bar{Z}$, $\bar{X}YZ$. These relations can then provide a way to check the orientation of the crystal in our goniometer.

Carbon-13 Results

Figure 1 shows a typical spectrum from a single crystal of glycine that was enriched to 9% with [1,2-$^{13}C_2$]glycine. The spectrum was taken with the magnetic field parallel to the *ac* plane, and therefore the resonances from all four molecules in the unit cell are expected to coincide. In this spectrum the downfield portion of the spectrum reveals a triplet from the carboxyl carbons consisting of a small central line due to the 1.1% natural abundance carbons, flanked by each line of a doublet which results from the dipolar coupling to the methylene ^{13}C in the enriched species. This three-line pattern is observed again with the methylene lines in the upfield portion of the spectrum and is split further by dipolar coupling to the neighboring ^{14}N nucleus into the observed triplet of triplets. In a general orientation, spectra from the two independent sites in the crystal will be observed, and therefore in the enriched crystals 6 carboxyl and 18 methylene lines will be observed. For the crystals that have not been enriched with ^{13}C, only the ^{13}C–^{14}N couplings are observed, and in a general orientation only two resonances are found for the carboxyl carbons and six for the methylene. The natural abundance methylene line positions as a function of crystal orientation are shown in Figure 2. One can immediately see from the *c* rotation in the lower half of the figure the predicted six lines for a general orientation, whereas only three lines are observed when the B_0 field is parallel to the *ac* plane (*b* rotation, upper half of Figure 2). Analysis of the splittings and line positions by standard methods[16] yields the dipolar and chemical shift tensors discussed in the following sections.

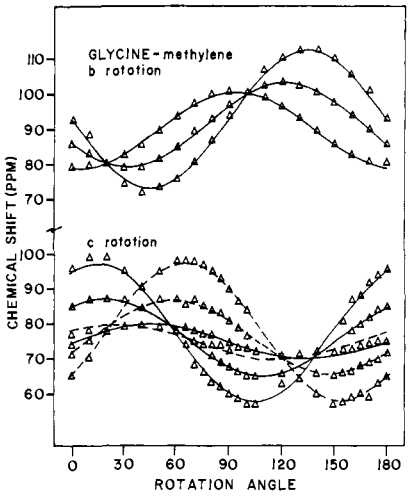

Figure 2. Rotation plots for the ^{13}C NMR spectra of the methylene carbons of glycine (natural abundance ^{13}C). Top: rotation about the *b* axis perpendicular to the field, B_0; bottom: *c* axis perpendicular to B_0. In the *c* rotation, lines from the two independent molecules are given by solid and dashed lines.

Table I. Glycine ^{13}C–^{14}N Dipolar Coupling Tensor Components and Their Direction Cosines for Each Independent Molecule of the Unit Cell

	principal values[a]	direction cosines[b]	reference direction cosines[b]
molecule 1	D_{11}	0.759	0.7580[c]
	−1.289 (0.017)	0.450	0.4462
		−0.470	−0.4726
	D_{22}	−0.490	−0.5543[d]
	0.573 (0.017)	0.871	0.8246
		0.043	−0.1130
	D_{33}	0.429	0.3393
	0.698 (0.017)	0.197	0.3478
		0.882	0.8740
molecule 2	D_{11}	0.743	0.7580[c]
	−1.278 (0.014)	−0.479	−0.4462
		−0.468	−0.4726
	D_{22}	0.420	0.5543[d]
	0.559 (0.014)	0.878	0.8246
		−0.231	0.1130
	D_{33}	0.521	0.3393[e]
	0.692 (0.014)	−0.024	−0.3478
		0.853	0.8740

[a] In kilohertz. Values in parentheses are standard deviations. [b] With respect to the a^*, *b*, *c* crystallographic axes. [c] Parallel to the C–N bond axis. [d] Perpendicular to the C–C–N plane. [e] Perpendicular to the C–N bond axis and in the C–C–N plane.

(14) P. G. Jönsson and A. Kvick, *Acta Crystallogr., Sect. B*, **28**, 1827 (1972).

(15) (a) "International Tables for X-Ray Crystallography", Vol. 1, Kynoch Press, Birmingham, England, 1952. (b) The equivalent positions from ref 15a for $P2_1/n$ are (x, y, z); $(\bar{x}, \bar{y}, \bar{z})$; $(x, y + {}^1/_2, z - {}^1/_2)$; $(x, y - {}^1/_2, z + {}^1/_2)$, but since NMR is not sensitive to translations, the pertinent symmetry elements are (x, y, z); $(\bar{x}, \bar{y}, \bar{z})$; $(x, \bar{y}, z)$; $(\bar{x}, y, \bar{z})$.

(16) G. M. Volkoff, H. E. Petch, and D. W. Smellie, *Can. J. Phys.*, **30**, 270 (1952); see also ref 2, pp 15–21.

Table II. Bond Distances and C-C-N Angle for Glycine Calculated from ^{13}C NMR Spectra and Compared with Neutron Diffraction Data

	this work	Jönsson and Kvick[14]
r_{CN}, Å	1.509 ± 0.009	1.490 ± 0.001
r_{CC}, Å	1.543 ± 0.008	1.539 ± 0.001
∠C-C-N, deg	111.1 ± 1.0	111.85 ± 0.05

^{13}C–^{14}N Dipolar Couplings

As shown in Figures 1 and 2, ^{13}C–^{14}N dipolar couplings can be readily extracted from the ^{13}C NMR spectra. Application of the second-order corrections used by Stoll et al.[9] would produce changes in the observed line positions of less than 10 Hz since the ^{14}N quadrupolar coupling is small (1.18 MHz; see below) and our B_0 field is large, 6.8 T. Corrections of such magnitude are lost in the line width and were therefore ignored. The principal values and direction cosines for the tensors of the dipolar coupling between the methylene ^{13}C and the ^{14}N are presented in Table I. Since dipolar tensors are always axially symmetric (in the absence of indirect coupling) about the bond axis, the dipolar splitting, $\Delta\nu$, can be expressed as[5]

$$\Delta\nu = \frac{\gamma_C\gamma_N h}{2\pi r_{CN}^3}(1 - 3\cos^2\theta) = D_{CN}\frac{1}{2}(1 - 3\cos^2\theta) \quad (1)$$

where r_{CN} is the CN bond length and θ is the angle between the internuclear vector and the external magnetic field, B_0, and γ_C and γ_N are the gyromagnetic ratios of ^{13}C and ^{14}N, respectively. Substituting for the constants we calculate D_{CN} to be

$$D_{CN} = 2.18086\ (\text{kHz}\cdot\text{Å}^3)\cdot r_{CN}^{-3}$$

After correcting for the scalar J_{CN} coupling,[17] we obtain from the data in Table I an average value of $D_{CN} = 0.635 \pm 0.011$ kHz ($D_{11} = -2D + J$, $D_{22} = D + J$, $D_{33} = D + J$). From this we derive $r_{CN} = 1.509 \pm 0.009$ Å (shown in Table II), compared with a value of 1.490 ± 0.001 Å obtained by Jönsson and Kvick[14] by neutron diffraction methods. The agreement between the two values is quite reasonable, especially considering that no corrections for the anisotropy of the J tensor or molecular vibrations were made. Since the J tensor transforms like the D tensor, the two are mathematically inseparable. In the case of $^{13}C^{14}N$ J couplings, the anisotropy is probably small and will not cause a large correction to r_{CN}. The vibrational corrections which were applied to the neutron data arise from the fact that the neutron methods determine $\langle r\rangle$, whereas the NMR technique yields $\langle r^{-3}\rangle^{-1/3}$. Each of these averages is performed over the vibrational displacements of the respective nuclei and therefore yields a different numerical value. The differences between the two values can be as high as 8–10% for very light nuclei such as protons,[18] but in the case of heavier nuclei such as ^{13}C and ^{14}N, the differences are probably, at most, 1%. Because the application of vibrational corrections requires a rather detailed knowledge of the molecular force field and is computationally lengthy, we chose to view as tolerable the 0.02-Å discrepancy between the NMR and diffraction results. In addition, we expect D_{11} to lie along the C–N bond axis but observe a deviation of about 3.4°. This discrepancy and also the observed asymmetry of our dipolar tensors may be partially attributed to anisotropic molecular motions but is most likely due to small errors in crystal alignment, goniometer inaccuracies, and/or diamagnetic susceptibility corrections to the chemical shifts.

It should be noted that observation of the direct dipolar coupling is by no means limited to directly bonded atoms but can sometimes be observed between more distant nuclei. Figure 3 shows a spectrum of natural abundance glycine oriented such that the b axis is perpendicular to the field and the carboxyl carbon–nitrogen vector is approximately parallel with the field. In this spectrum,

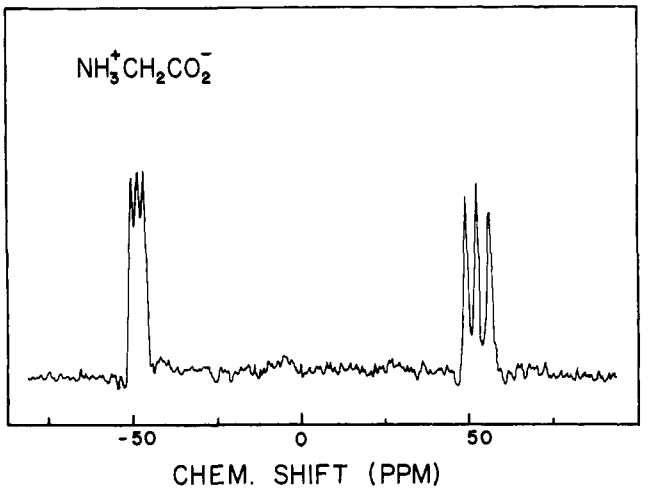

Figure 3. ^{13}C NMR spectrum of natural abundance glycine. The b axis is perpendicular to the field B_0, and the $^-O_2C\cdots NH_3^-$ vector is almost parallel with B_0.

Table III. Glycine ^{13}C–^{13}C Dipolar Coupling Tensor Components and Their Direction Cosines for Each Independent Molecule of the Unit Cell

	principal values[a]	direction cosines[b]	reference direction cosines[b]
molecule 1	D_{11}	0.035	0.0320[c]
	−4.126 (0.047)	0.132	0.1568
		0.990	0.9871
	D_{22}	0.870	0.8317[d]
	2.025 (0.047)	−0.493	0.5435
		0.035	−0.1133
	D_{33}	0.493	−0.5543[e]
	2.184 (0.047)	0.860	0.8246
		−0.132	−0.1130
molecule 2	D_{11}	0.034	0.0320[c]
	−4.155 (0.049)	−0.194	−0.1568
		0.981	0.9871
	D_{22}	0.844	0.8317[d]
	1.986 (0.049)	0.531	−0.5435
		0.075	−0.1133
	D_{33}	−0.536	0.5543[e]
	2.157 (0.049)	0.825	0.8246
		0.182	0.1130

[a] In kilohertz. Values in parentheses are standard deviations. [b] With respect to a^*, b, c crystallographic axes. [c] Parallel to the C–C bond axis. [d] Perpendicular to the C–C bond and in the C–C–N plane. [e] Perpendicular to the C–C–N plane.

the carboxyl resonance, which should normally consist of only one line, is split into a triplet by dipolar coupling to the ^{14}N nucleus, about 2.484 Å distant. This splitting is nearly maximal (260 Hz) in this orientation and normally manifests itself only as a line broadening; therefore, we obviously could not determine a complete dipolar tensor. However, observation of the splitting indicates that in favorable circumstances longer range couplings might be measured in sufficient detail to determine structural parameters.

^{13}C–^{13}C Dipolar Couplings

As mentioned previously, use of ^{13}C-enriched glycine crystals enabled us to observe direct ^{13}C–^{13}C dipolar couplings in the ^{13}C NMR spectrum. The dipolar tensors were determined from these data by the same methods used for the ^{13}C–^{14}N data and are presented in Table III. The tensors are traceless and very nearly axially symmetric ($(D_{22} - D_{33})/D_{11} \approx 0.03$). For the case of two ^{13}C nuclei with different chemical shifts, eq 1 reduces to

$$D_{CC} = 7.59105\ (\text{kHz}\cdot\text{Å}^3)\cdot r^{-3}$$

Using the data in Table III we obtain an average $D_{CC} = 2.066$

(17) $J_{^{13}C^{15}N} = 6.3$ Hz from ^{13}C NMR of an aqueous glycine solution. (calcd $J_{^{13}C^{14}N} = 4.5$ Hz). $J_{^{13}C^{13}C} = 53.1$ Hz from ^{13}C NMR of aqueous glycine solution.

(18) S. Sykora, J. Vogt, H. Bosiger, and P. Diehl, *J. Magn. Reson.*, **36**, 53 (1979).

Table IV. Glycine Methylene ^{13}C Chemical Shift Tensor Principal Values and Direction Cosines for Each Individual Molecule of the Unit Cell

	principal values[a]	direction cosines[b]	ref axes[b]
molecule 1	σ_{11}	−0.333	−0.5543[c]
	63.1 (0.8)	0.920	0.8246
		−0.204	−0.1130
	σ_{22}	0.787	0.7066[d]
	82.2 (0.8)	0.391	0.5381
		0.478	0.4594
	σ_{33}	0.519	0.4396[e]
	101.8 (0.8)	−0.001	0.1748
		−0.855	−0.8810
	82.4 (0.5) ppm = (1/3)Tr(σ)		
molecule 2	σ_{11}	0.396	0.5543[c]
	61.6 (0.8)	0.883	0.8246
		0.252	0.1130
	σ_{22}	0.763	0.7066[d]
	83.7 (0.8)	−0.469	−0.5381
		0.446	0.4594
	σ_{33}	−0.512	−0.4396[e]
	101.7 (0.8)	−0.015	0.1748
		0.859	0.8810
	82.3 (0.5) ppm = (1/3)Tr(σ)		

[a] In ppm from external C_6H_6. Values in parentheses are standard deviations. [b] With respect to a^*, b, c crystallographic axes. [c] Perpendicular to N–C–C plane. [d] Bisects N–C–C angle in N–C–C plane. [e] Perpendicular to c and d to form a right-handed system.

± 0.034 kHz (corrected for J_{CC} = 53.1 Hz[17]) and a C–C bond distance of 1.543 ± 0.008 Å (Table II) in excellent agreement with the value of 1.539 ± 0.001 Å determined by Jönsson and Kvick.[14] Again the NMR data are not corrected for molecular vibrations nor the anisotropy of the J tensor. In this case an anisotropy in the J tensor of only 100 Hz could account for the observed 0.004-Å discrepancy. D_{11} lies within 1.7° of the C–C bond axis. From the direction cosines for D_{11} in Tables I and III we calculate an average C–C–N bond angle of 111.1 ± 1.0° which again agrees very well with the value of 111.85° determined by diffraction. The excellent agreement of these data demonstrates the utility of dipolar couplings for determining bond distances and angles in crystalline solids.

^{13}C Chemical Shift Tensors

Spectra such as those in Figures 1 and 3 also yield ^{13}C chemical shift tensors for both carboxyl and methylene carbons; these values are derived by standard methods[16] from the angular behavior of the centers of gravity of each multiplet. Although the shift tensors for both the natural abundance and enriched crystals were determined, the two sets of results were identical within experimental error and we therefore present only one set of tensors.

Methylene Shift Tensors

The principal components and direction cosines for the methylene ^{13}C chemical shift tensors are presented in Table IV. The principal values are similar to those observed for other methylene shift tensors.[19-21] However, comparison of these values reveals that although the anisotropy and asymmetry of the tensor is typical of methylene carbons, the isotropic shift is somewhat downfield owing to the deshielding propensity of the ammonium and carboxyl groups. The orientation of each component is also fairly typical and reflects the approximate C_{2v} symmetry of the CH_2 moiety. However, Figure 4 shows that slight differences do exist owing to the perturbing influence of the $-NH_3^+$ and $-CO_2^-$ groups. As

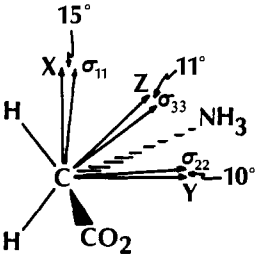

Figure 4. Orientation of methylene ^{13}C chemical shift tensors in glycine. The XYZ system was chosen so that X is perpendicular to the NCC plane, Y is in this plane and bisects the HCH angle, and Z is orthogonal to these directions.

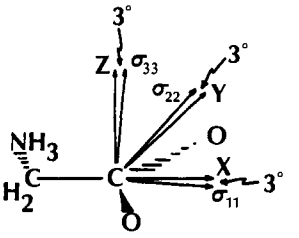

Figure 5. Orientations of carboxyl ^{13}C chemical shift tensors in glycine. The XYZ system shown was chosen so that X is in the CO_2 plane and bisects the OCO angle, Z is perpendicular to the CO_2 plane, and Y is orthogonal to these directions.

Table V. Glycine Carboxyl ^{13}C Chemical Shift Tensor Principal Values and Direction Cosines for Each Independent Molecule of the Unit Cell

	principal values[a]	direction cosines[b]	ref axes[b]
molecule 1	σ_{11}	0.055	0.0321[c]
	−118.8 (0.6)	0.111	0.1445
		0.992	0.9890
	σ_{22}	0.950	0.9649[d]
	−52.9 (0.6)	0.299	0.2537
		−0.086	−0.0684
	σ_{33}	−0.307	−0.2607[e]
	25.9 (0.6)	0.948	0.9564
		−0.089	−0.1313
	48.6 (0.4) ppm = (1/3)Tr(σ)		
molecule 2	σ_{11}	0.034	0.0321[c]
	−119.7 (0.8)	−0.165	−0.1445
		0.985	0.9890
	σ_{22}	0.990	0.9649[d]
	−48.6 (0.8)	−0.129	−0.2537
		−0.055	−0.0684
	σ_{33}	0.136	0.2607[e]
	22.5 (0.8)	0.978	0.9564
		0.159	0.1313
	48.6 (0.4) ppm = (1/3)Tr(σ)		

[a] In ppm from external C_6H_6. Values in parentheses are standard deviations. [b] With respect to the a^*, b, c crystallographic axes. [c] Bisects O–C–O angle. In O–C–O plane. [d] Perpendicular to c and to O–C–O plane. [e] Perpendicular to O–C–O plane. Forms a right-handed system.

can be seen, σ_{22} nearly bisects the N–C–C angle and is tilted out of the NCC plane by about 10°. σ_{11}, which is usually found normal to the NCC plane, is inclined by 15° toward the nitrogen atom.

Carboxyl Shift Tensors

The principal values for the $-CO_2$ group, which are presented in Table V, are similar to those found in malonate[19] and other unprotonated carboxylic acids,[22] but somewhat different than those observed for oxalate.[11] While σ_{11} and σ_{33} are in all cases ap-

(19) J. J. Chang, R. G. Griffin, and A. Pines, *J. Chem. Phys.*, **62**, 4923 (1975).
(20) D. L. VanderHart, *J. Chem. Phys.*, **64**, 830 (1976).
(21) S. Pausak, J. Tegenfeldt, and J. S. Waugh, *J. Chem. Phys.*, **61**, 1338 (1974).

(22) See ref 2, p 185.

Table VI. Glycine ^{14}N Quadrupole Coupling Tensor Principal Values and Their Direction Cosines for Each Independent Molecule of the Unit Cell

	principal values[a]	direction cosines[b]	ref direction cosines[b]
molecule 1	V_{XX}	−0.500	−0.5543[c]
	−0.414 (0.010)	0.857	0.8246
		0.128	−0.1130
	V_{YY}	0.430	0.3393[d]
	−1.314 (0.010)	0.117	0.3478
		0.895	0.8740
	V_{ZZ}	0.752	0.7580[e]
	1.776 (0.010)	0.503	0.4462
		−0.427	−0.4726
molecule 2	V_{XX}	0.543	0.5543[c]
	−0.423 (0.010)	0.810	0.8246
		−0.220	0.1130
	V_{YY}	0.428	0.3393[d]
	−1.370 (0.010)	−0.042	−0.3478
		0.903	0.8740
	V_{ZZ}	0.722	0.7580[e]
	1.771 (0.010)	−0.585	−0.4462
		−0.370	−0.4726

[a] In megahertz. Values in parentheses are standard deviations. [b] With respect to a^*, b, c crystallographic axes. [c] Perpendicular to C–C–N plane. [d] Perpendicular to C–N bond and in C–C–N plane. [e] Parallel to C–N bond axis.

proximately −120 and +25 ppm, respectively, the main difference between the two classes of acids is the value of σ_{22}. In the case of diammonium oxalate it is about −30 ppm, whereas for most other acids, such as malonate, σ_{22} is around −50 ppm. Glycine falls into this latter category with σ_{22} = −50.8 ppm.

The orientation of the principal components is shown in Figure 5. σ_{11} lies approximately along the bisector of the O–C–O angle (~3°), σ_{22} is approximately coplanar (~3.2°) with the O–C–O plane, and σ_{33} is nearly perpendicular (~3.3°) to this plane. This is quite typical of carboxylic shift tensors.

Nitrogen-14 Results

Since ^{14}N has spin I = 1 and therefore a quadrupole moment, the nuclear Hamiltonian for a solid sample in high B_0 fields is usually dominated (after the Zeeman term) by the quadrupolar interaction rather than the chemical shift.[13,23] This interaction is the coupling between the quadrupole moment of the nucleus, eQ, and the electric field gradient at the nucleus, eqV and manifests itself by shifting the $(2I + 1)$ Zeeman energy levels so that the high-field NMR spectrum consists of $2I$ separate resonances spaced at frequency intervals given by the quadrupolar coupling. Thus, for each magnetically inequivalent ^{14}N two lines are observed separated in frequency by

$$\Delta\nu_Q = \frac{3e^2qQ}{4h}((3\cos^2\beta - 1) + \eta\sin^2\beta\cos 2\alpha)^{23} \quad (2)$$

where e^2qQ/h is the quadrupole coupling constant and α and β are the Euler angles describing the orientation of the quadrupole coupling tensor in the magnetic field. η is the asymmetry parameter and is defined as

$$\eta = (V_{YY} - V_{XX})/V_{ZZ}$$

where V_{ii} are the principal components of the electric field gradient tensor and we adopt the convention here that $|V_{ZZ}| \geq |V_{YY}| \geq |V_{XX}|$. In addition the tensor must be traceless. A typical ^{14}N NMR spectrum of a glycine crystal is presented in Figure 6 and shows the four expected resonances from the two inequivalent nitrogens in the unit cell. Because of the extreme breadth of most ^{14}N NMR spectra of solids (in this case ~1.5 MHz), the spectra were obtained in four 100-kHz sections as the finite bandwidth, and pulse power of our spectrometer precluded obtaining the entire spectrum with one free induction decay. The variation of the line positions, as the crystal is rotated with the magnetic field always parallel to the ab plane, is shown in Figure 7. Reduction of these data yields the tensors for each independent molecule presented in Table VI and whose orientation is shown in Figure 8. In each case the tensors are traceless and yield a nuclear quadrupole coupling constant of e^2qQ/h = 1.182 ± 0.010 MHz and an asymmetry parameter of η = 0.54 ± 0.01. The largest component V_{ZZ} lies nearly along the C–N bond and V_{XX} is almost perpen-

(23) See ref 5, Chapter VII, and ref 2, p 8.

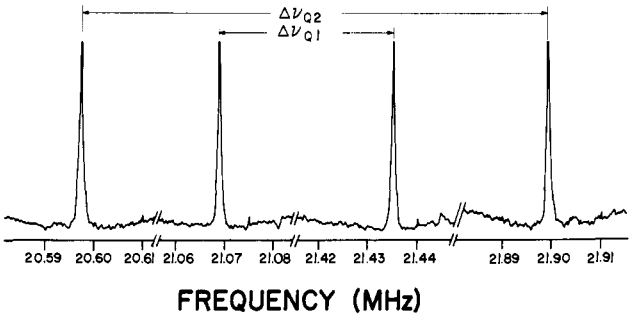

Figure 6. ^{14}N NMR spectrum of glycine. The c axis is perpendicular to B_0. Line widths are about 600 Hz and typical of those observed in NH_3^+ groups. The spectrum was taken in four 100-kHz sections as the bandwidth of our spectrometer did not permit the observation of the complete spectrum simultaneously.

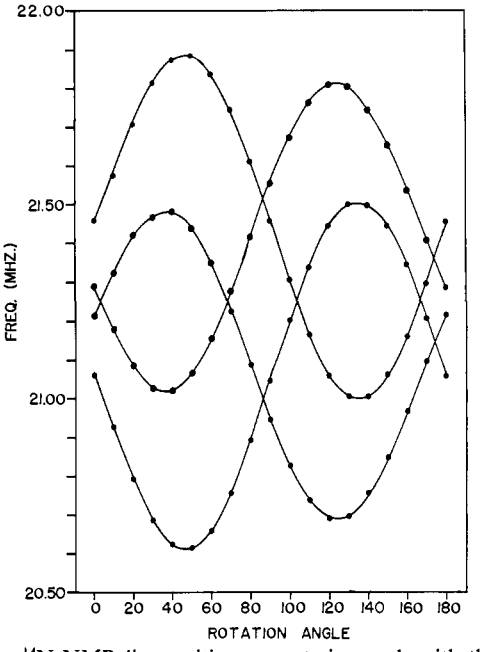

Figure 7. ^{14}N NMR line positions vs. rotation angle with the c axis perpendicualr to B_0. Note the ~1.5-MHz splittings observed.

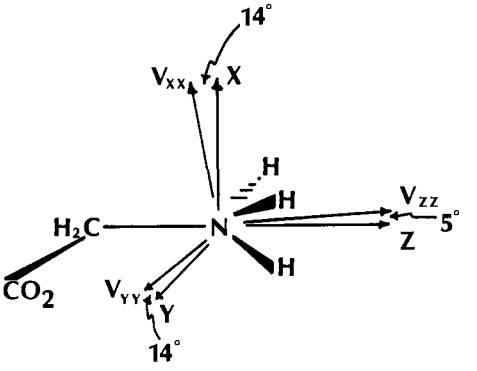

Figure 8. Orientation of the ^{14}N quadrupole coupling tensors in glycine. The XYZ system was chosen so that X is perpendicular to the C–C–N plane, Y is perpendicular to the C–N bond and in the C–N plane, and Z is parallel to the C–N bond axis.

dicular to the NCC plane. These results are in good agreement with an early study by Anderson et al.[25] who obtained e^2qQ/h = 1.247 ± 0.001 MHz, η = 0.5 ± 0.1 at room temperature. However, they are somewhat different from those observed by Edmonds et al.,[26] who found e^2qQ/h = 1.247 ± 0.001 MHz, η = 0.502 ± 0.003, and strikingly different from the measurements of Blinc et al.[27] who obtained e^2qQ/h = 0.745 MHz, η = 0.61. The differences among the reported values for e^2qQ/h and η are probably due to the widely different temperatures at which the experiments were performed. Both Edmonds et al. and Blinc et al. employed indirect detection methods in their experiments, and for these experiments to function properly the spin–lattice relaxation rates in the proton spin reservoir must be correct. In order to satisfy this constraint, Edmonds, et al. worked at 77 K, and Blinc et al. performed their experiments at 413 K, which are respectively 210° lower and 115° higher than the temperature at which our measurements were performed. Thus, it seems likely that lattice vibrations which will suffice to average the ^{14}N electric field gradient tensor are absent at lower tempertures and present at room and higher temperatures. Therefore, our data and those of Blinc et al. probably reflect a degree of averaging because of this type of motion. This hypotheses is further supported by the fact that we find V_{ZZ} to be very near to the C–N bond as might be expected, whereas Blinc et al. report that at 413 K V_{ZZ} makes an angle of about 60° with the direction of this bond. Note that this averaging process due to lattice motion should be distinguished from the more commonly observed molecular reorientation processes like hopping $-CF_3$ groups or flipping H_2O or D_2O molecules. In the latter cases the shift or quadrupole tensor reorients with respect to the laboratory field when the $-CF_3$ group hops by 120° or when the D_2O molecule flips by 180° and the ^{19}F, ^1H, or ^2H spectrum manifest these effects. However, in the case of an $-NH_3^+$ group, reorientation about the C–N bond will not strongly affect the ^{14}N tensor. In particular, hydrogen bonding in the lattice determines the distortions of the $-NH_3^+$ moiety from C_{3v} symmetry and thus governs the size and asymmetry of the electric field gradient tensor. If the lattice does not move and if the reorientation process is slow compared to electronic relaxation times, then a 120° hop of the $-NH_3^+$ group will not affect the ^{14}N tensor. Thus, the only way to motionally average this tensor is via lattice vibrations as suggested above, and these must be fast compared to about 10^6 Hz.

As noted by previous investigators,[24-27] the relatively high symmetry of the NH_3^+ group produces a ^{14}N quadrupole coupling in glycine which is significantly smaller than that found for >NH or $-NH_2$ groups, but larger than the coupling observed for the more symmetrical NH_4^+ ion.[13,24-27] Note also that because of the high degree of symmetry present in the $-NH_3^+$ moiety, the maximum splittings are actually quite moderate in size; in fact, in several cases (e.g., peptide nitrogens) the ^{14}N NMR spectrum is spread over about 5 MHz.[10,13] The line widths in the latter cases increase by a factor of 2–3 over the 600 Hz observed in Figure 6.[10,24] While these line widths might at first seem prohibitive, they are invariably accompanied by dramatic increase in the frequency range over which the resonances occur. As a consequence the resolution in ^{14}N spectra is actually greater by about two orders of magnitude than that usually obtained, for example, in high-resolution ^{13}C solution studies of large molecules. Therefore, ^{14}N NMR seems to be a promising technique with applications to many areas of biology, chemistry, and physics.

Finally, we should also mention that we have also observed ^{15}N spectra of glycine and found that they consist of a line of 300-Hz breadth, indicating that the ^{15}N shift tensor is ~10 ppm. Similar results have been obtained for $-NH_3^+$ groups in other cases as well.

Conclusions

The NMR studies presented here demonstrate that dipolar interactions between spin pairs which are dilute in a crystal lattice can provide meaningful structural information and represent the only technique other than diffraction methods that can directly provide such information in the solid state. In all spectroscopic and diffraction methods used for measuring atomic distances the equilibrium internuclear separation, r_e, is not obtained directly, but instead an average distance which is averaged over the vibrational modes of the molecule. In the case of the dipolar couplings this averaging process yields $\overline{\langle r^{-3}\rangle}^{-1/3}$ which may be significantly different from r_e for lighter nuclei. However, as we have seen from the results in Table II, the differences between $\overline{\langle r^{-3}\rangle}^{-1/3}$ and r_e obtained for bond distances between heavier nuclei such as ^{13}C and ^{14}N are fairly small and may not cause any serious limitations in many applications. Therefore, the use of dipolar couplings to determine bond distances and angles is a practical alternative, particularly when one desires the structure of only a small portion of a larger molecule.

In addition, we have also demonstrated two important facets of single-crystal ^{14}N NMR. First, because of its 99.4% abundance it is quite easy to obtain acceptable signal-to-noise ratios in ^{14}N spectra in rather short periods of time. In addition, the resolution in these spectra is about two orders of magnitude greater than that obtainable in ^{13}C NMR. Thus, in principle, it should be possible to study small crystals of relatively large molecules with this technique. Since nitrogen has the ability to form hydrogen bonds and is often involved in important chemical functions, ^{14}N NMR provides an appealing and direct way to examine structural problems related to nitrogen-containing compounds. The single disadvantage of ^{14}N experiments at present is a technical one, and that is because the spectra span such a large frequency range that they must be taken in sections. However, this is a problem that can be circumvented with suitable spectrometer modifications.

Acknowledgment. This research was supported by the National Institutes of Health through Grants GM-23403 and RR-00995 and by the National Science Foundation through Contract C-670 to the Francis Bitter National Magnet Laboratory. R.E. Stark acknowledges the support of an NIH postdoctoral fellowship (AI-05634).

(24) R. E. Stark, R. A. Haberkorn, and R. G. Griffin, (submitted for publication).
(25) L. O. Anderson, M. Gourdji, L. Guibe, and W. G. Proctor, *C.R. Acad. Sci.*, **267**, 803 (1968).
(26) D.T. Edmonds, *Phys. Rep.* **29C**, 233 (1977).
(27) R. Blinc, M. Mali, R. Osredkar, A. Prelesnik, I. Zupančič, and L. Ehrenberg, *Chem. Phys. Lett.*, **9**, 85 (1971).